An Application of LARY_C: Discrete Wavelet Transform Applied to Heart Rate Variability Analysis. Assessment of the Autonomic Nervous System Behaviour in Control and Iron-Deficient Anemic Infants

Claire Médigue, Julie Bestel, Sophie Renard, Jean Clairambault, Marcelo Garrido, Felipe Pizarro, Patricio Peirano

INRIA

INSTITUT NATIONAL DE RECHERCHE EN INFORMATIQUE ET EN AUTOMATIQUE

An application of LARY_C: discrete wavelet transform applied to heart rate variability analysis. Assessment of the autonomic nervous system behaviour in control and iron-deficient anemic infants

Claire Médigue, Julie Bestel, Sophie Renard, Jean Clairambault, Marcelo Garrido,

Felipe Pizarro and Patricio Peirano

N ° 3203

Juillet 1997

THÈME 4

Rapport de recherche

ISSN 0249-6399

INRIA
ROCQUENCOURT

An application of LARY_C: discrete wavelet transform applied to heart rate variability analysis. Assessment of the autonomic nervous system behaviour in control and iron-deficient anemic infants

Claire Médigue, Julie Bestel, Sophie Renard, Jean Clairambault, Marcelo Garrido, Felipe Pizarro and Patricio Peirano

Thème 4 — Simulation et optimisation
de systèmes complexes
Projet Sosso

Rapport de recherche n ° 3203 — Juillet 1997 — 40 pages

Abstract: Our aim was to assess the Autonomic Nervous System (ANS) behaviour in six months old iron-deficient anemic and control infants during sleep.
We used LARY_C, a software package, developped in the synchronous, data flow, parallel language SIGNAL, primary dedicated to the ANS analysis, through the study of physiological signals and their correlations.
We applied the discrete wavelet transform to heart rate variability analysis, which reflects the SNA activity. The method provides suitable frequency resolution in low frequency domain, which is precisely of physiological interest.
Significant differences between iron-deficient and control infants are shown in both quiet and active sleep, suggesting an autonomic dysfunction or delay in iron-deficient anemic infants.

Key-words: time-frequency method, discrete wavelet transform, synchronous language, autonomic nervous system, physiological signals, heart rate variability, sleep, iron deficiency anemia

(Résumé : tsvp)

Dr. Patricio Peirano, Felipe Pizarro and Marcelo Garrido are with Unidad de neurofisiologia del desarrollo, INTA - Universidad de Chile

Unité de recherche INRIA Rocquencourt
Domaine de Voluceau, Rocquencourt, BP 105, 78153 LE CHESNAY Cedex (France)
Téléphone : (33) 01 39 63 55 11 – Télécopie : (33) 01 39 63 53 30

Une application de LARY_C: la transformée en ondelettes discrète appliquée à l'analyse des variabilités du rythme cardiaque pour l'étude du système nerveux autonome chez des enfants controles et anémiques par carence en fer

Résumé : Notre but était d'étudier l'impact de la carence en fer sur le comportement du Système Nerveux Autonome (SNA) de bébés de six mois pendant le sommeil, en comparant deux groupes, l'un contrôle et l'autre atteint d' anémie par déficience martiale.
Nous avons utilisé LARY_C, logiciel développé dans le langage synchrone flot de données et parallèle SIGNAL, essentiellement dédié à l'étude du SNA, à travers l'analyse des rythmes physiologiques et de leurs corrélations.
Nous avons appliqué la transformée en ondelettes discrète à l'analyse des variabilités du rythme cardiaque, reflet de l'activité du SNA. Cette méthode donne une bonne résolution fréquentielle dans le domaine des basses fréquences, qui sont précisément les fréquences d'intérêt physiologique.
Des différences significatives sont apparues entre les bébés carencés en fer et les bébés contrôles, pour chacun des stades de sommeil calme et agité; ceci suggère un dysfonctionnement ou un retard de développement du SNA chez les bébés anémiques par déficience en fer.

Mots-clé : méthodes temps-fréquence, transformée en ondelette discrète, language synchrone, système nerveux autonome, signaux physiologiques, variabilité cardiaque, sommeil, anémie, carence en fer

Contents

1 Introduction

This study is carried out on six months old infants, control and anemic, during a nap. We wanted to assess the influence of Iron Deficiency Anemia (IDA) on the Autonomic Nervous System (ANS) maturation according to sleep states.

This study, as part of an ECOS-CONICYT programme between France and Chili, is made in collaboration with INTA - University of Chili (department of neurophysiology on developpment).
The Iron Deficiency Anemia (IDA) continues to be the most common single nutrient deficiency in the world. About 20 to 25% of the infant population worldwide is affected [1]. Several recent studies provide strong evidence that IDA alters infant development and behaviour [7, 8]. Recent research on developmental patterns of Heart Rate Variability (HRV) provide measures that are thought to reflect central nervous system functioning earlier and more closely than tests of mental and motor development [2, 3, 4]. Indeed, the HRV reflect the control of the ANS, and the resulting HRV patterns reflect the continuous feedback between the central nervous system and peripheral autonomic receptors. The ANS is the part of the Nervous system involved in regulating all the vital functions, particularly the cardio-vascular and respiratory systems, to maintain the vital balance and to allow the organism to adapt to changes in its state. The ANS has two components (sympathetic and parasympathetic (vagal)) which have an antagonist effect on the heart; the balance between these two components varies in function of sleep and waking states; in quiet sleep, the parasympathetic tonus is dominant whereas in active sleep a lot of sympathetic stimulations of different origins arise.
The study of the Heart Rate (HR) and it's variabilities is already well known as a noninvasive mean of investigating the ANS [24]. The HRV being a function of sleep states, it is so necessary to separately study the heart rate during quiet sleep and active sleep. On the raw rhythms, only the global, resulting effects of the two components, of the ANS balance are seen. On the HR, for example, the global effect of a sympathetic activation is an acceleration, whereas the effect of a parasympathetic activation is a deceleration. It is possible to describe more precisely the participation of each composant of the ANS, through HR variabilities (HRV) (Fig. 12). Among the frequencies bands known to reflect the ANS activity, one can consider:

- An high frequency band (HF): "Heart rate fluctuations at respiratory frequencies are recognized as a noninvasive measure of cardiovagal activity and reflect more modulation of firing of baroreceptors and of cardiac and pulmo-

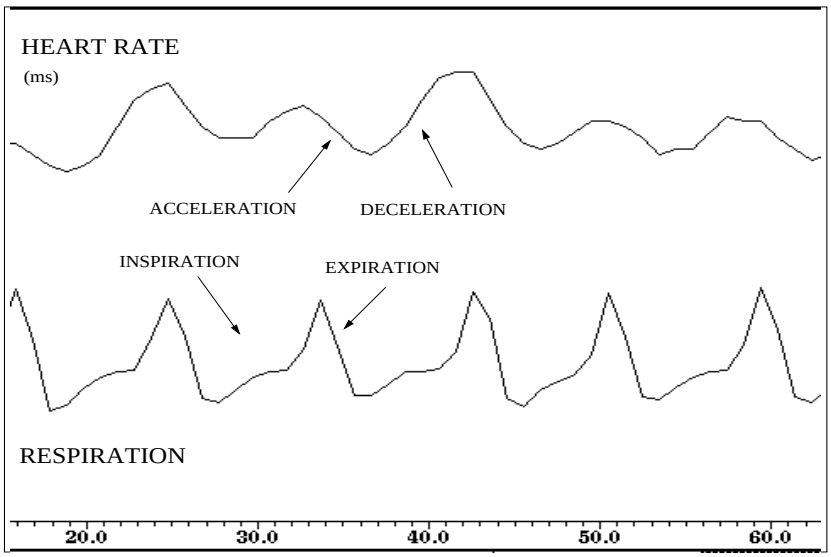

Figure 1: Respiratory Sinus Arrhythmia visualised on the heart rate and the raw respiratory signal, together resampled at 4Hz

nary volume receptors than an absolute measure of vagal tone" [6].
Above 0.15 Hz, it reflects the parasympathetic tone alone; on the HR, it is called Respiratory Sinus Arrhythmia (RSA) and it is the part of variability related to the respiratory cycles; RSA is described as an increase in heart rate during inspiration and a decrease during expiration (Fig. 1). Within mechanisms involved, the blockade of the centrally generated inspiratory drive and the blockade of lung receptors during inspiration are responsible for a phasic vagal inhibition [17].

- A middle frequency band (MF): Between 0.03 and 0.15Hz, it is related to the cardio-vascular control of the ANS, through the arterial baroreceptors; changes in heart rate and in peripheral vasomotor regulation are involved. The two ANS components, sympathetic and parasympathetic, have an antagonist chronotrope effect on the heart rate whereas the vasomotor activity involves the sympathetic effect on vessel contraction; the baroreflex activity, called Mayer waves, concerns periods about 10 heart beats and gives a peak rather around 0.1Hz in adult. As baroreflex responses derive from interactions between multiple reflex inputs, the situation is very complex and the frequential activity could be increased toward 0.1Hz in case of dominant vagal influence ; conversely, it could be reduced toward 0.05Hz in case of dominant sympathetic influence, with a strong peripheral vasoconstriction [24].
- Low and very low frequency bands (LF and VLF): lower frequency bands reflect probably not only the autonomic control and are involved in mechanisms of thermoregulation, variations in plasma hormones, including catecholamines, angiotensine ...

We used the Discrete Wavelet Transform (DWT) to analyse these heart rate variabilities, as it is developped in the medical library of LARY_C. Our aim is to rely on the high frequential resolution improved by the DWT to compare the HRV of anemic and control infants.

2 The wavelet transform

2.1 Recall: basics on the spectrogram

The spectrogram is a classical time-frequency analysis tool that has been widely performed on non-stationnary signals:

$$S_f(t,\nu) = \left| \int_{-\infty}^{+\infty} \hat{f}(n)\hat{h}(n-\nu)e^{2i\pi nt}dn \right|^2 \quad (1)$$

where $\hat{f}(n), n \in \mathbb{R}$, denotes the Fourier transform of $f \in L^2(\mathbb{R})$. As shown by eq.(1), it simply consists in scanning the frequency domain by shifting a unique lowpass filter. Assuming that h is an analysing window with equivalent time-support Δt and bandwith B, it provides a tiling of the time-frequency plane with uniform cells of fixed dimensions Δt and $\Delta f = B$, the product $\Delta f \Delta t$ being constant and lower bounded (according to Heisenberg-Gabor's incertitude principle). Now, let us focus on another analysis tool, based on the wavelet transform.

2.2 Continuous wavelet transform

Let $\Psi(t)$ be a function with good time and frequency localization properties. It has to fulfill the admissibility condition $\hat{\Psi}(0) = \int_{\mathbb{R}} \Psi(t)dt = 0$, and it is then called the mother wavelet. We define the family of its dilated and time shifted versions

$$\left\{\psi_{(a,b)}(t) = \frac{1}{\sqrt{a}}\ \Psi\ \left(\frac{t-b}{a}\right), b \in \mathbb{R}, a \in \mathbb{R}_+^*\right\}$$

One then defines the CWT of f as the expansion of f onto the analysing set $\left\{\psi_{(a,b)}\right\}$:

$$C_f(a,b) =< f, \psi(a,b) >= \int_{-\infty}^{+\infty} f(t)\overline{\psi}_{(a,b)}(t)dt \tag{2}$$

(a,b) taking on values in the half plane $\mathbb{R}_+^* \times \mathbb{R}$. $C_f(a,b)$ is a time-scale representation of f.

2.3 Filtering interpretation

When dealing with finite energy signals: $f \in L^2(\mathbb{R})$, we have:

$$\int |f(t)|^2 dt = \frac{1}{C_\Psi} \int\int \frac{|C_f(a,b)|^2}{a^2} dadb$$

where C_Ψ is a coefficient of normalization dependent on Ψ (see [10]). Given the admissibility condition, Ψ is band-limited with bandwith B and central frequency ν_0; then its dilated version $\Psi(t/a)$ has a spectrum centred around ν_0/a with bandwith B/a. The convolutive structure entering the definition of CWT (eq.(2))1 results in a Q-constant filter bank analysis, where $Q = \frac{B}{\nu_0}$. Therefore, the CWT yields a frequency-dependent tiling of the time-frequency plane: Δf and Δt vary depending on a (one at the expense of the other) while mantaining the product $\Delta f \Delta t$ constant; it thus provides good frequency resolution in low frequencies. However, the CWT is informationally redundant, since it is a transformation from $L^2(\mathbb{R})$ to $L^2(\mathbb{R}^2)$.

2.4 Discrete transform

To reduce the redundancy of the CWT, a discrete version has been proposed. Loosely speaking, the DWT can be understood as a CWT sampled on a discrete grid of the (a,b) plane. A dyadic grid is commonly proposed: $a = 2^j, b = 2^j k$ where $j \in \mathbb{Z}^*, k \in \mathbb{Z}$. This particular tiling corresponds to a critical sampling of the time-scale

plane that ensures no loss of information and possible reconstruction. Moreover, I. Daubechies showed that it was possible to find compact-supported orthonormal bases yielding discrete decomposition, which guarantees no loss of energy through the whole expansion [11]. A similar frequency interpretation as for the CWT holds for the DWT: given a signal sampled at F_s Hz, the wavelet at scale j acts as a bandpass filter between $F_s 2^{j-1}$ Hz and $F_s 2^j$ Hz. Besides reduction of redundancy, DWT allows efficient and fast algorithms.

2.5 Implementation

A fast implementation was proposed by S. Mallat [10]. Its principle is depicted in figure 2. G and H are respectively highpass and lowpass filters that form a Quadrature Mirror Filters pair ([12]). Downsampling by a factor of 2 allows using the same filters at each resolution level, and therefore leads to an iterative structure: the so-called pyramidal algorithm. Convolutions were computed by Radix FFT multiplications followed by IFFT. The wavelets used are orthonormal compact-supported Daubechies wavelets. At each scale j, the quantities displayed are normalized $\left|C_f(2^j, 2^j k)\right|^2$, and will now be referred to as Discrete Wavelet Coefficients (DWC).

3 Clinical material and methods

3.1 Subjects

Fifteen control and fifteen iron deficient anemic infants, 6 to 7 months old were studied. The healthy subjects are defined according in particular the following criteria: birth weight $\geq$ 3.0 Kg, singleton birth, no congenital or neonatal complications or anomalies, and no other nutrient deficiency. The diagnostic of iron-deficient anemia was based on biological criteria (as hemoglobin $\leq 103 g/l$) and subsequently on an increase in hemoglobin level of 10 g/l or more in response to iron therapy. The research protocol was approved by the Institutional Review Boards of the University of Michigan Medical Center, Ann Arbor, and of INTA, University of Chile, Santiago.

3.2 Recording

3.2.1 General procedure

Standard polygraphic recordings were conducted in the sleep laboratory of the Developmental Neurophysiology Unit, INTA, University of Chile. They were performed

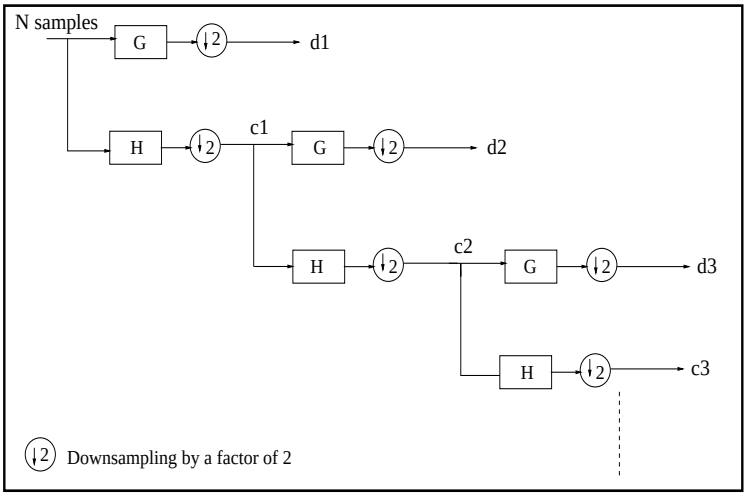

Figure 2: Pyramidal algorithm

during a spontaneous afternoon nap, in standardized conditions to limit the influences of environment, circadian rythms and food intake on sleep-waking patterns and related physiological activities.
Data were digitized at 250 Hz and simultaneously recorded on paper tracings and stored on optic disk.
Electrocardiogram (ECG) and respiratory signal were automatically analysed; concerning breathing, abdominal respiratory movements using a mercury strain jauge and nostril airflow using a thermistor were recorded.
Sleep states were visually determined. They were related with ECG and respiratory signals by the mean of a file including the time of the state change and it's nature. Correspondence between paper tracings and digitized recordings was ensured by a time counter in LARY_C: beside sleep state changes, it allowed also to locate special events , as rocking in the mother arms, which have to be discarded from the automatic analysis.

3.2.2 Coding sleep states

They were visually coded by the concordance of behavioral and electrophysiological criteria [8, 9], which are extracted from the electro-encephalographic (EEG), electro-oculographic (EOG) and electro-myographic (EMG) signals.

- Quiet sleep: eyes closed, no eyes movements, EEG patterns with predominant delta waves with or without spindles.
- Paradoxical state: eyes closed, rapid eyes movements, muscular atonia, predominant high frequency and low voltage EEG patterns nd irregular respiration.
- Indeterminate sleep: mixed characteristics of the two previous states.

4 Signal processing

The approach given by LARY_C depends on two points: the use of the synchronous language SIGNAL to analyse relationships between rhythms and the library of medical signal processing methods to construct these rhythms.

4.1 Environment

4.1.1 The SIGNAL language

SIGNAL is a data flow, oriented synchronous language for describing relationships among signals at various sampling rates; signals are sequences of events with associated values. The conception of time in SIGNAL is a minimal one, serving only to describe an application in a determinist way (same computations always run in the same order); in particular, no duration is considered at this level. The discrete time associated with a signal is called the 'clock' of the signal. The relationships among events are:
- precedence: occurrences of a same signal are totally ordered;
- simultaneity: two occurrences of different signals may be simultaneous or not;
- functional: values associated with simultaneous events may by linked by a computation expression.
SIGNAL provides a small set of temporal operators, sufficient for expressing all kinds of synchronization relationships among the clocks of the signals.
The application may be seen as a directed graph; arcs represent signals and dependancies between inputs and outputs of the nodes; a node express temporal and functional constraints of the signals that it connects. The SIGNAL compiler verifies

the global coherence of this complex relational system, and builds the corresponding automaton for a target machine [13, 18, 19, 20, 21].

4.1.2 LARY_C

We elaborated a complete processing chain in LARY_C, a software package for physiological rhythms analysis, previously described. [21, 27] ; LARY_C is based on the SIGNAL industrial environnement of development , SILDEX [1]. LARY_C is supported by UNIX and X Windows. The flow chart of the whole parallel processing for this application is shown on Fig.3; it is divided into the following steps:

Cardio and respiratory rhythms detection A parallel preprocessing of the raw signals gives the resulting rhythms:
- From the electro-cardiographic signal (ECG) to the heart rate (HR)
The first processing step is the extraction of the different rhythms: a QRS detection adaptative algorithm is applied on the ECG, then an equidistant resampling at 4 Hz [14] is applied on the heart rate (HR).
- From the respiratory signal, the instantaneous respiratory frequency is calculated by differenciation of the analytical signal.

Heart rate processing The Discrete Wavelet Transform, used as a time-frequency method, studies the heart rate variabilities. This analysis is done by 1024 points epochs.

Cardio-respiratory parameters extraction The delivered results are the HR (mean RR, DWC) and respiratory (frequency) variables averaged over 1024 points epochs (4.2 mn), in relation with the current sleep state.

4.2 Description of the global processing

4.2.1 ECG signal processing

From the ECG signal, we extract the heart rate. The different steps of the whole heart rate processing are represented in the Fig. 6, as they are implemented in LARY_C.
The raw ECG is prefiltered with a Finite Impulse Response filter (FIR), in order to

[1] TNI,Technopôle Brest-Iroise, ZI du Vernis, 29608 Brest Cedex (France)

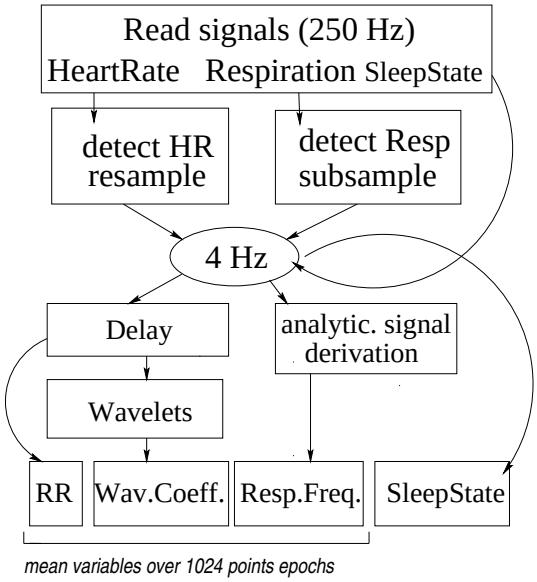

Figure 3: Flow chart of the parallel signal processing

derivate it and to reinforce the QRS complexes (Fig. 5). The detection is based on the correlation between the filtered ECG and the filter response whose shape is a derivated QRS: each time a detection occurs, the response is modified by the current QRS derivated complex on the ECG (eq. 3); the filter response is initialized with a derivated QRS shape and the forgetting factor$a$ is fixed to 0.1 [27, 19].

$$\text{response}[i] = a * \text{response}[i-1] + (1-a) * QRS'[i] \tag{3}$$

An adaptative threshold detects the R peaks and returns the RR signal or heart rate; this RR signal is the serie of the distances between two R peaks, e.g. the number of ECG samples between two R peaks; this distance is usually translated in ms. This heart rate is in fact an unregularly sampled signal. An equidistant resampling [14] at 4Hz is applied (Fig. 6). Then an artefact detection is used, based on a clinical criterium of beat-to-beat variability: a RR can't be different from the previous one by more than 25%. An artefact so detected is replaced by the average of the n last valid RR. This method parameters have to be adjusted to each recording to make a compromise between the respect of the variability and the necessary detection of

the artefacts (Fig. 7).

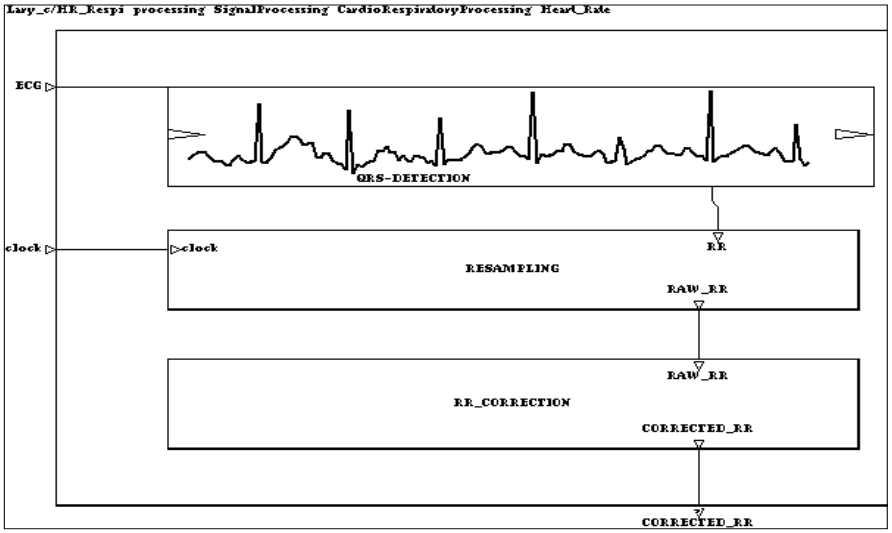

Figure 4: The modules of LARY_C for Heart Rate processing, in the SILDEX graphical environnement
The 3 steps are the following ones:
- the QRS detection from the ECG to calculate the RR intervals or Heart Rate
- the Heart Rate resampling at 4Hz
- the detection and correction of the artefacts

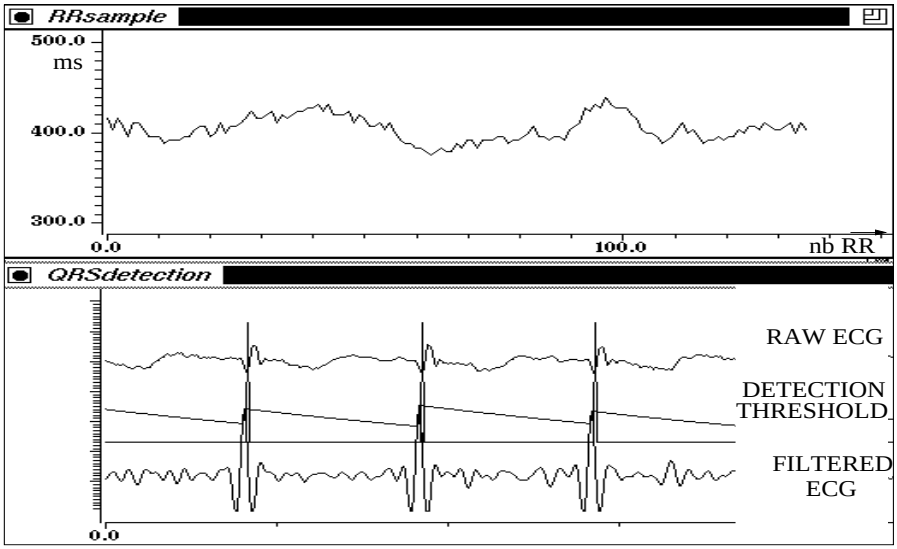

Figure 5: Illustration of the first step of the HR processing: the QRS detection
On the QRS detection screen (bottom), one can see the filterd ECG with the adaptative threshold; the vertical lines cutting the QRS complexes represent the events of detection; the distance between two detections (in number of ECG samples) is converted in ms and reported on the y axis of the RR signal screen (top).

4.2.2 Respiratory signal processing

The instantaneous respiratory frequency is calculated by differentiation of the analytical signal (Fig. 8); this signal is obtained by a fIR-filter which computes the imaginery part (dephasing of 90 degrees); the domain where the filter is applicable is [.01-.49] normalised frequency. The frequency is the derivative of the arctangent of the analytical signal (Fig. 9). An illustration of the resulting signals is done in Fig. 10. We did'nt take into account the amplitude of the respiratory (module

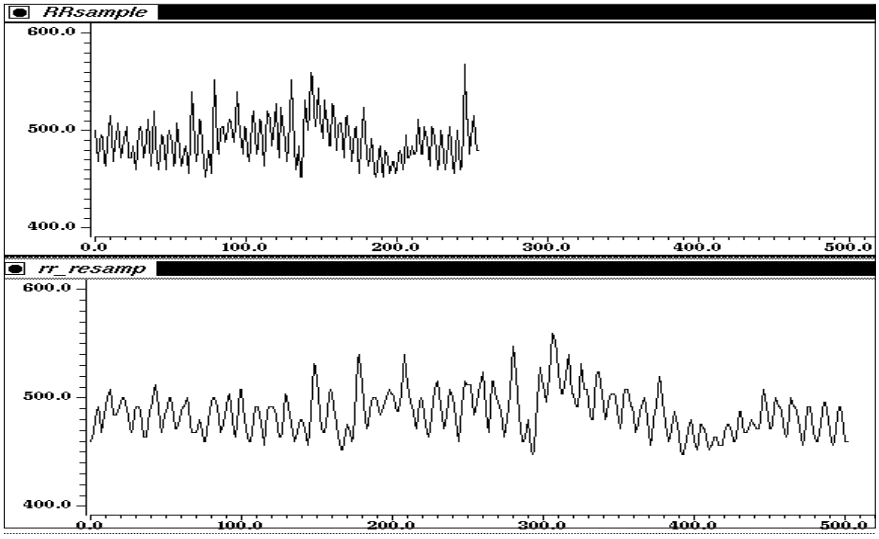

Figure 6: Illustration of the second step of the HR processing: resampling at 4Hz
The HR is expressed in ms; on the top, the raw RR signal, approximatively around 2Hz (the mean RR is 500ms); on the bottom, the resampled RR signal; the x axis are expressed in number of RR samples.

of the analytical signal) because of the incertitude about the gains of the different recordings.

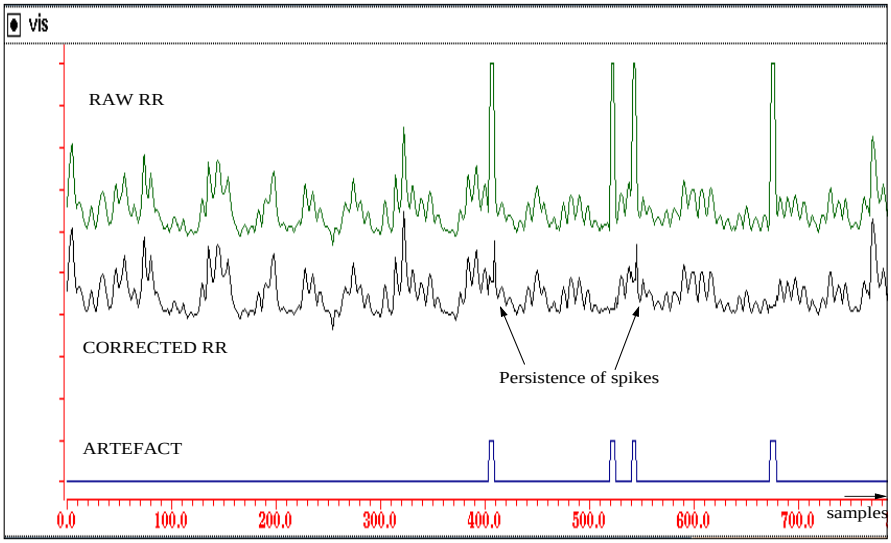

Figure 7: Illustration of the third step of the HR processing: detection and correction of the artefacts
This screen shows the effects due to the compromise between the respect of the variability and the necessary detection of the artefacts; in this case, the detection threshold was fixed at a high rate not to smooth the real variability; but it induced the persistence of spikes.

4.2.3 DWT applied to HRV analysis

Relations between wavelet coefficients and classical frequency bands Table 1, Fig.11 and Fig.12 show the correspondence between DWC and the periods of physiological interest; c2 and c3 include the RSA, c4 and c5 the cardiovascular control; in particular, c4 closely contains the Mayer waves, corresponding to 10 heart beat periods.

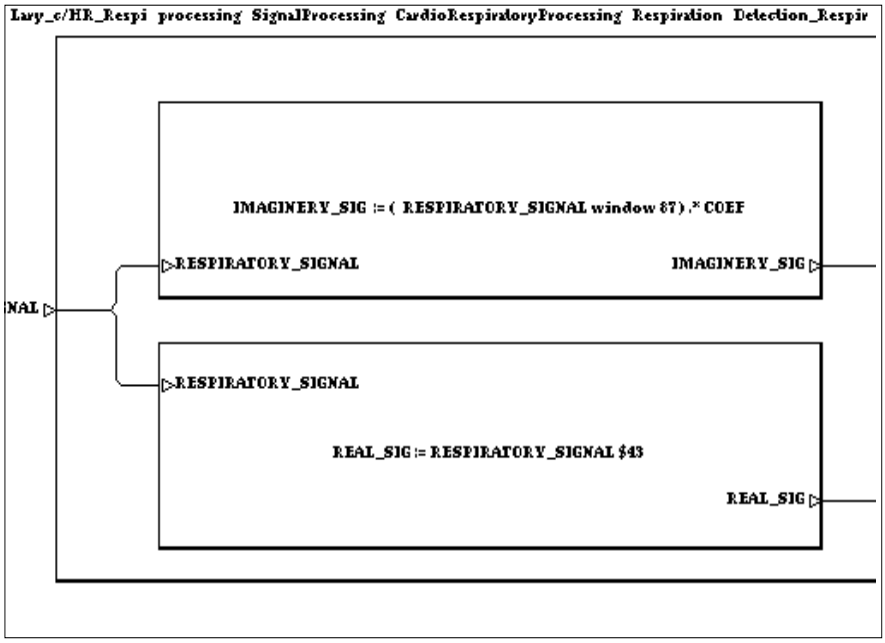

Figure 8: Respiratory signal processing: computation of the analytical signal in the SIGNAL language

The imaginery part is computed by a FIR filter (dephasing of 90 degrees), with 87 coefficients; the delay induced by this filter is of 43 samples ($(n-1)/2$) and it can be compensated on the real part of the signal by the SIGNAL operator $.

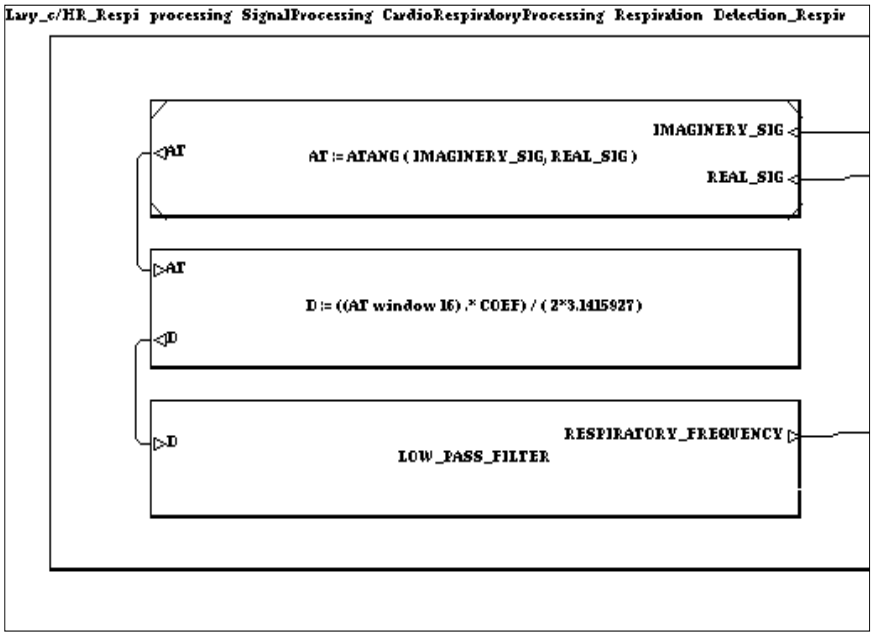

Figure 9: Respiratory signal processing: computation of the instantaneous respiratory frequency in the SIGNAL language

The arc-tangent of the analytical signal is derivated by a FIR, then low-pass filtered to produce the respiratory frequency.

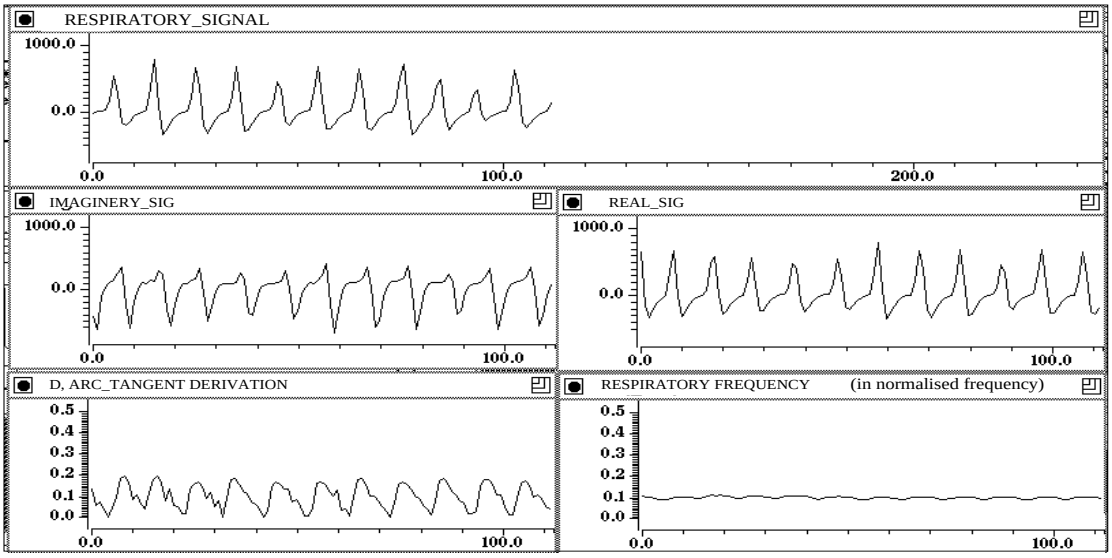

Figure 10: Respiratory signal processing: illustration of the different signals represented in the previous Fig.

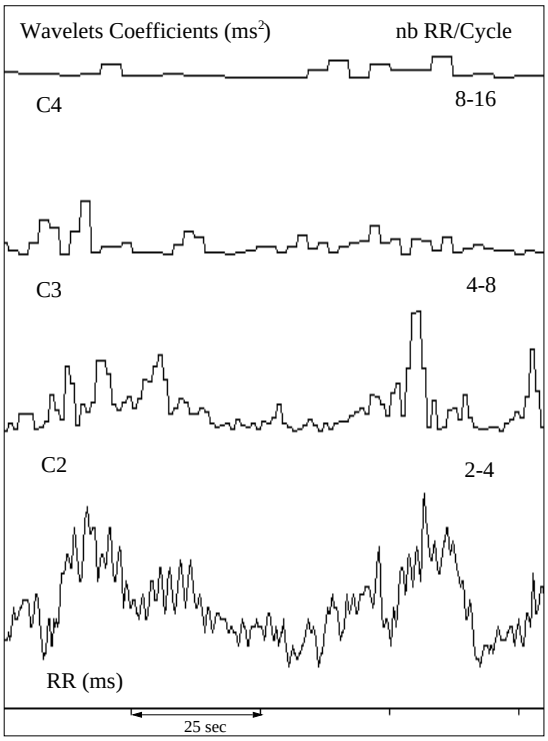

Figure 11: The first Discrete wavelet coefficients, corresponding to HF and MF

4.3 Some pratical aspects

4.3.1 Synchronisations between resulting rhythms

They were all resampled at 4Hz (Fig. 3) to be processed together and resynchronised because the different processing steps introduce delays; this was done by using filters with a linear phase, producing a constant time delay which can be exactly known. The Fig. 8 shows the details of implementation in the SIGNAL language. After resynchronisation, an averaging is done over the cardiac and respiratory variables; these variables are: heart rate, discrete wavelet coefficients, from C2 to C8, respiratory frequency. These means constitute the statistical units; they are done

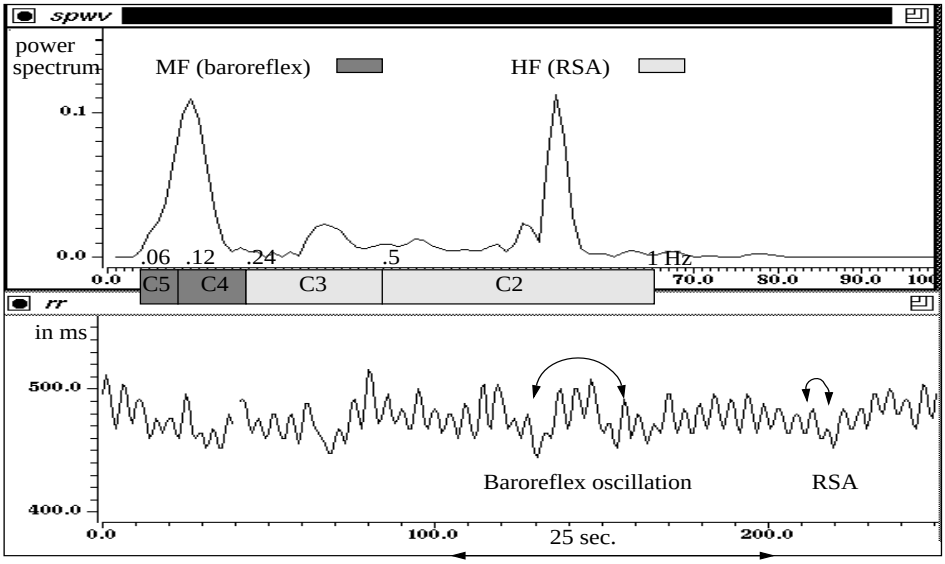

Figure 12: Correspondence between time and frequency representations of the heart rate

A low-pass filter avoided the low frequencies to focuse on the two frequency bands HF and MF; for this baby, the MF peak is centered on .16Hz, that corresponds to periods around 12 heart-beats; the HF peak is around .7Hz, that corresponds to periods around 3 heart-beats. The DWC are reported onto the spectrum to show the correspondence between the different representations.

Table 1: Discrete wavelet coefficients and frequencies

DWC	N.Freq.	Freq. (Hz)	Period ($nbRR$)	Freq. Bands
c2	.125 .25	.5 .1	2 4	HF
c3	.062 .125	.24 .5	4 8	
c4	.031 .062	.12 .24	8 16	MF
c5	.015 .031	.06 .12	16 32	
c6	.007 .015	.028 .06	32 64	LF
c7	.003 .007	.012 .028	64 142	&
c8	.001 .003	.004 .012	142 285	VLF

N.Freq.:normalized frequency

each 1024 samples (about 4.2mn), which represent the window lenght for the wavelet processing; this size was chosen to get a good enough frequential resolution in low frequencies, according to the Heisenberg-Gabor's incertitude principle.

4.3.2 Visual criteria

Table 2: Methods parameters

Parameters	Values
Sampling frequency on raw signals	250 Hz
Resampling frequency on resulting rhythms	4 Hz
Window length for means	1024 samples, 4.26 mn

Table 2 summarises the main parameters used in the signal processing chain. The respiratory frequency was detected in parallele with the DWC of the heart rate and averaged each 1024 samples; they are together displayed on the screen (Fig.13); this allowed us to follow the real respiratory frequency and to verify that it never slowed towards the Mayer waves [5]. For all the 30 recordings, the averaged respiratory frequency calculated from the raw respiratory signal is included between .35 and .7 Hz, that corresponds to C2 and C3. This visual inspection of the processing also allowed us to discard from the study the epochs with remaining artefacts,

except short spikes affecting only the first DWC as it is shown on Fig.14. These precautions and the lenght of the unit observation explain that in AS, where heart rate is very disturbed by artefacts, only 7 infants remain in each group compared to the (15 infants in each group).

5 Statistical processing

5.1 Classical hypothesis tests

They were performed on the variables averaged within one subject to assume independence of observations. We choose non parametric hypothesis tests, adapted for a few samples. Among them, the between-groups differences, control versus anemic, within the same sleep state were assumed by the unpaired Mann-Whitney'U test (its parametric equivalent is the t-test unpaired). The between-state differences within the same group were assumed by the non parametric test of Wilcoxon which is a paired test, comparing differences within the same subject (its parametric equivalent is the t-test paired).

5.2 Mutivariate Data Analyses (MDA)

We choose the most significant variables at the classical hypothesis tests to perform the following analysis: Principal Component Analysis (PCA), Linear Discriminant Analysis (LDA) and Factorial Discriminant Analysis (FDA). Their principle is based on the choice of the best linear combination of the chosen variables to describe a population and to explain the contribution of each of them in the between-groups discrimination.
For the Principal component analysis (PCA), as it is a purely descriptive method which makes no assumption on the statistical properties of the variables, all the 4 mn epochs were represented.

6 Clinical results

6.1 Between-group differences in Quiet Sleep

In QS (15 anemic v. 15 control), the addition of c2 and c3, corresponding to the global ASR, is significantly enhanced in control infants (Tab. 3, Fig 16). The DA, using the linear combination of HF(c2,c3) and LF(c7,c8) (c4,c5,c6 were not

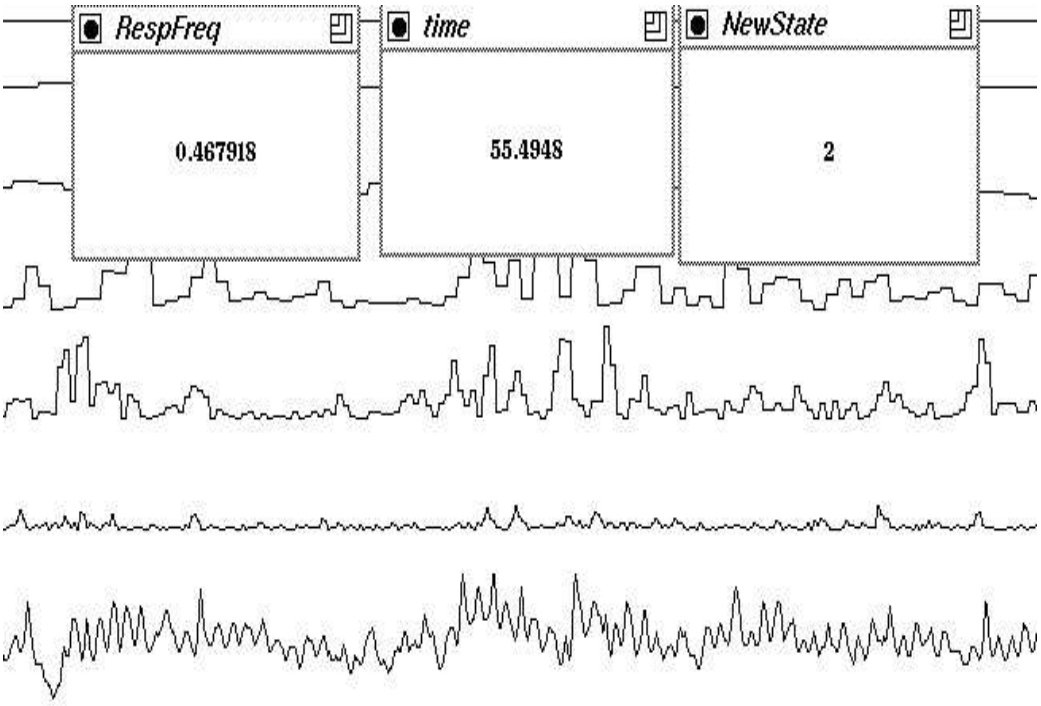

Figure 13: The Wavelet application on the Heart Rate during execution

This view represents a part of the 1024 HR samples, unit of the wavelet processing; for each 1024 points epoch, the HR signal and it's wavelet coefficients, the mean respiratory frequency, the current sleep state (number 2 for QS) and the time (in mns) of the end of the epoch are displayed on the screen. So, it is possible to verify that C2 and C3 really contain the RSA.
From bottom to top, HR, C1 to C8; C1 was not of interest for this study.

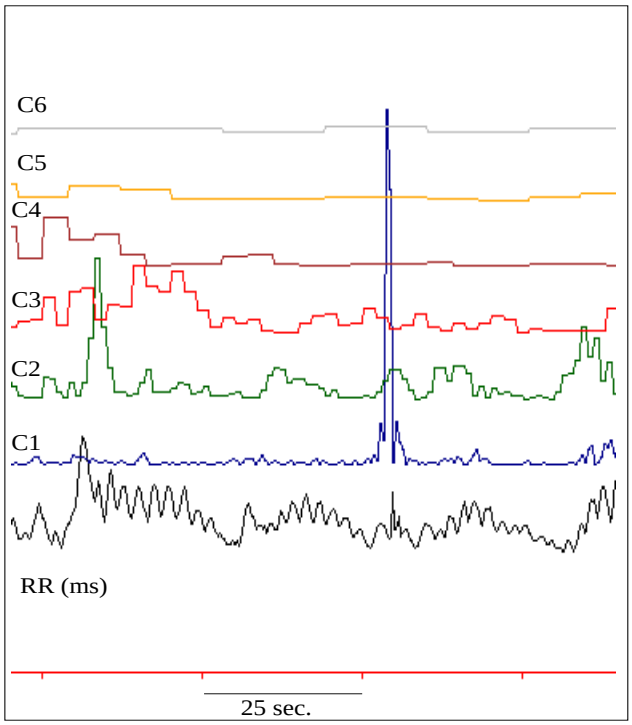

Figure 14: Effect of an HR artefact on the Discrete Wavelet coefficients
The spike on the HR is responsible for a very high frequency event which perturbs only the first coefficient; this one having no interest in physiological variabilities.

relevant for discrimination) does'nt allow a very well discrimination (65% after cross-validation) but the correlation coefficient of the discriminant linear form (DLF, which provides the decision rule) shows the opposition between HF and LF (Tab. 4), as seen on the principal factor plane ($>$ 80% global variance) of the PCA. The first factor (x axis) represents the HF and LF powers with negative correlations whereas the second factor (y axis) represents the HF-LF opposition, with negative correlations for HF, positive for LF. Anemic and control are separated along these two axes.

Table 3: Between-group differences in Quiet Sleep

DWC (ms^2)	control mean	StD	anemic mean	StD	Mann-Whytney U test
c2+c3	77	68	50	65	$p \leq .03$ *
c2	33	28	22	21	$p \leq .07$
c3	44	46	28	46	$p \leq .04$ *

n:15 in each group; *: $p \leq .05$

Table 4: Correlation of DLF with DWC in Quiet Sleep

HF		LF	
c2	+.614	c7	-.143
c3	+.498	c8	-.404

6.2 Between-group differences in Active Sleep

In AS (7 anemic v. 7 control), c4, corresponding to baroreflex activity, is significantly enhanced in anemic infants (Tab. 5, Fig. 17) . The DA using the MF(c4,c5) and a part of LF(c6) coefficients (the others are not relevant for discrimination), allows a discrimination of 78.6 %, with the strongest correlation of the DLF for c4 (-.93). No significant between-group differences were found in mean RR or in respiratory frequency, neither in AS nor in QS.

Table 5: Bewteen-group differences in Active Sleep

DWC (ms^2)	control mean	StD	anemic mean	StD	Mann-Whitney U test
c4	6.2	3.9	12	6.7	$p \leq .04$ *

n: 7 in each group

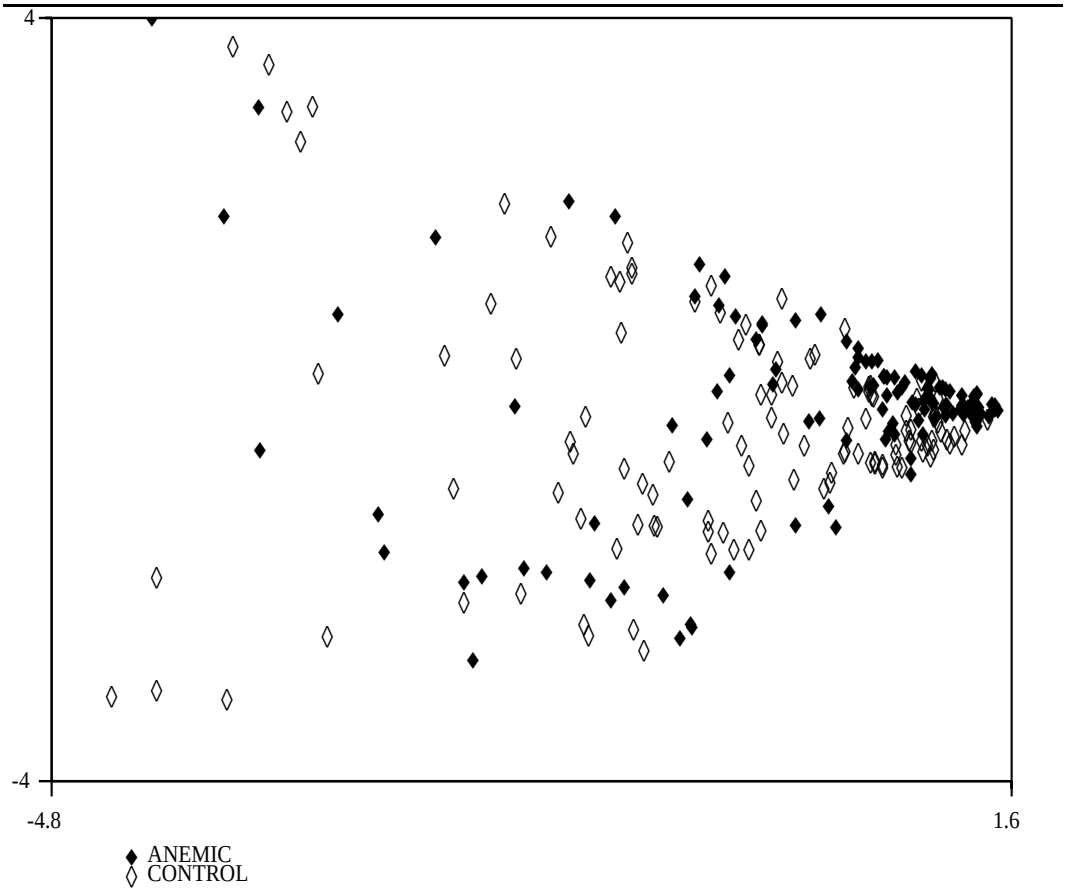

Figure 15: Principal component analysis in Quiet Sleep
Projection of all the 4mn HR epochs (125 control/125 anemic) onto the principal factor plane, according to the linear combination of HF (c2,c3) and LF (c7,c8) coefficients.
x = *-.59 c2 + -.64 c3 + -.74 c7 + -.71 c8*
y = *-.67 c2 + -.61 c3 + .52 c7 + .71 c8*

6.3 Between-state differences in each group

In the control group, QS and AS are significantly opposed by c2, enhanced in QS and c8, enhanced in AS (Tab 6). The DA, based on the HF(c2,c3)/LF(c7,c8) coefficients

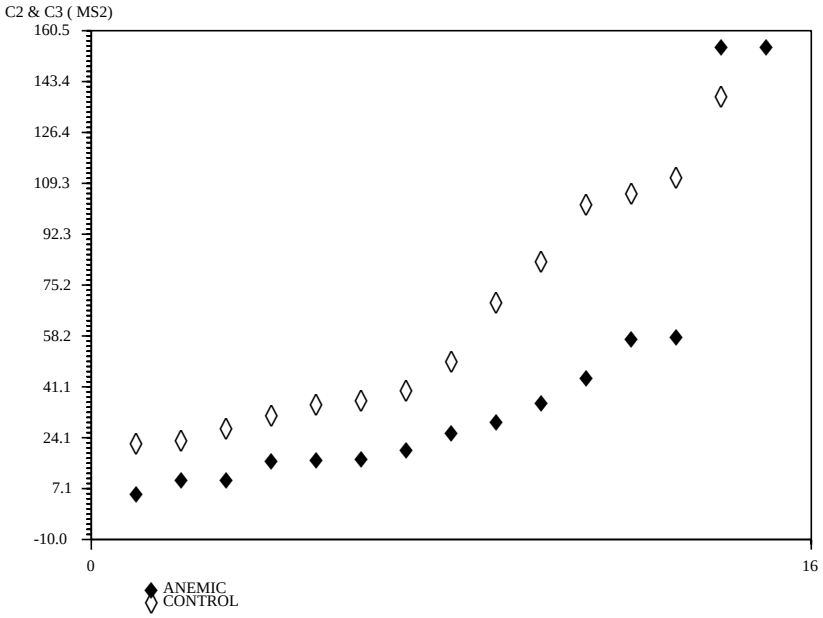

Figure 16: Between-group differences in Quiet Sleep: Discrete Wavelet Coefficients C2 and C3 corresponding to RSA
The DWC of 15 anemic (black diamond) versus 15 control (white diamond) infants are plotted by growing order along the x axis; each point represents the mean value of the C2 and C3 coefficients for one baby.

allows a discrimination of 82 %, and the correlation coefficient of the DLF with the DWC shows the HF/LF opposition (Tab. 8). The mean RR has a nearly significant enhancement in QS ($p \leq .06$, 495 v. 465ms). In the anemic group, neither significant differences (except almost for c4) nor conspicuous results in LDA appeared (Tab 6).

7 Discussion

7.1 About signal processing methods

Previous studies used other time and time-frequency methods: the Short Time Fourier Transform (STFT), applied to HRV of newborns [35, 34, 16]; the Smooth Pseudo

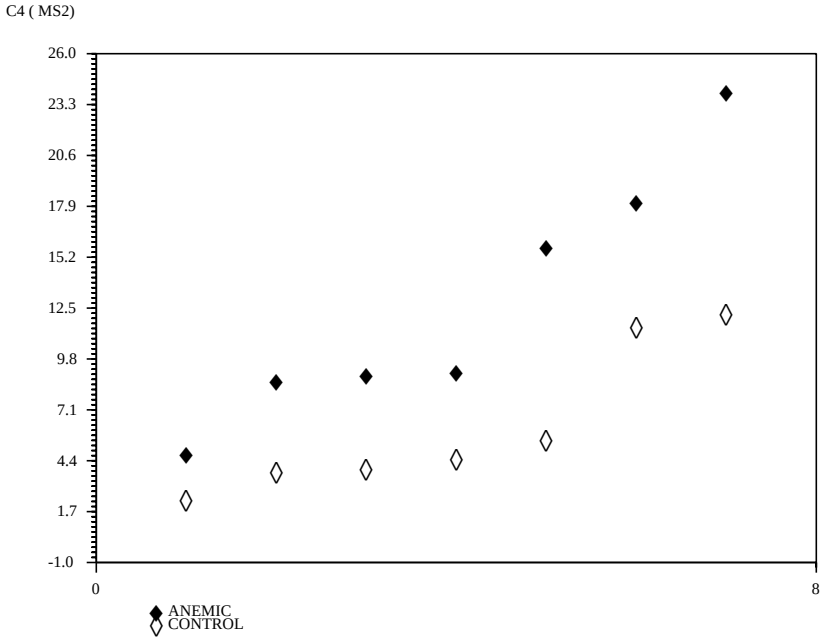

Figure 17: Between-group differences in Active Sleep: Discrete Wavelet Coefficient C4 corresponding to baroreflex activity
The DWC of 7 anemic (black diamond) versus 7 control (white diamond) infants are plotted by growing order along the x axis; each point represents the mean value of the C4 coefficients for one baby.

Table 6: Between-sleep-states differences in control infants

DWC (ms^2)	AS mean	AS StD	QS mean	QS StD	Wilcoxon test
c2	**17**	**12**	**27**	**17**	p $\leq$ .02 *
c4	6.2	3.9	7.0	4.0	NS
c8	**.31**	**.20**	**.14**	**.05**	p $\leq$ .02 *

n=7; NS: non significant; *: p $\leq$ .05

Wigner-Ville Transform (SPWVT) applied to HRV of transgenic mice and Periodic

Table 7: Between-sleep-states differences in anemic infants

DWC (ms^2)	AS mean	AS StD	QS mean	QS StD	Wilcoxon test
c2	25	20	30	28	NS
c4	12.6	6.7	7.8	6.2	$p \leq .06$
c8	.47	.48	.25	.23	NS

n=7; NS: non significant; *: $p \leq .05$

Table 8: Correlation of DLF with DWC in control infants

HF		LF	
c2	+.442	c7	-.271
c3	+.388	c8	-.680

Leg Movement Syndrome [31, 30, 33]; the cardio-respiratory Modified Complex Demodulation (MCD) [29, 28, 32, 33].
With SFT and SPWVT, the power spectrum is divided into several frequency bands, based on a physiological interpretation; the previous studies defined HF as periods from 2 to 8 heart-beats, MF from 10 to 25, and LF from 30 to 100. On the opposite, with the DWT used here, we try to give a physiological explanation to pre-fixed dyadic coefficients. So, some differences appeared (Tab.1), especially a very precise frequency band around Mayer Waves (8-16 heart-beats).
STFT doesn't allow a very good frequential definition, especially in low frequencies; SPWVT is more precise but interferences inherent in the method, compel us to avoid low frequencies and to limit the study to HF and MF. The MCD was used to study the HF only, in following the respiratory influence on the heart rate.
With DWC the frequential definition is well suited to low frequencies; with regard to this point, the window length of 1024 samples was chosen to get a good enough frequential resolution, according to the Heisenberg-Gabor's incertitude principle.

7.2 About Statistical methods

Even if great care is necessary to interpret the results, especially in active sleep, the same statistical methodology was already used for published studies [16, 34, 35];

they involved few individuals (8 full-term newborns, 8 intermediate, 8 premature). Concerning this study, 15 control versus 15 anemic infants in quiet sleep, 7 control versus 7 anemic infants in active sleep were the subject of the tests. The non-parametric tests are suitable for few samples and/or no Gaussian distribution; from six-seven individuals, the equivalence tables with parametric tests give reliable results. The discriminant analyses theoretically assume normality but are robust enough to tolerate violations of this normality assumption [36, 37].
We fixed the data window length at 1024 samples (about 4mn), which appeared to us as a good duration for an observation unit to take within subject variance into account. This variance effect is well shown by Principal Component Analysis, which uses all the epochs; it is made possible because the PCA is purely descriptive and makes no assumption on the statistical properties of the variables. On the opposite, the hypothesis tests were performed on the means over the epochs within one subject in a given sleep state to guarantee the independance of the observations.

7.3 About clinical results

We will try to explain the results of this study, particularly why the differences found between anemic and control infants don't involve the same neuro-vegetative variables in quiet and in active sleep.
In quiet sleep, anemic infants have a lower parasympathetic tone than controls, which confirms a previous study [32] and a not yet published work by P. Peirano. In active sleep, anemic infants have a greater sympathetic stimulation, in the range of the Mayer waves, than the control ones. This result is not yet confirmed (but not invalidated) by the previous study of P. Peirano. An explanation can be the very precise frequency definition around the Mayer Waves (from 8 to 16 heart-beats), given by the wavelet transform whereas the previous study used a larger frequency band (from 10 to 25 heart-beats). Nevertheless, the data are not exactly the same and the results remain to be confirmed on a larger population. In control infants only, results evidence the different levels of the autonomic balance according to sleep states: dominance of the parasympathic tone in QS versus the sympathic one in AS.

To each sleep-waking state corresponds a particular physiologic state [38, 39]. A reciprocal interaction exists between the mechanisms which control the sleep-waking states and those which control the vegetative functions ("Carotide" comes from "to doze off" (karoun in greek), illustration of the hypnogenic effect of the baroreflex regulation).

7.3.1 Influence of the sleep on the neurovegetative functions

The QS is a state of very low metabolic consumption, with a maximal stability of the vegetative functions. The SA is a state under a "behavioral"control, motor perturbations (body or facial movements) modulate the respiratory and baroreflex control. In AS especially, two patterns, which can be evaluated on chin muscle [40] are considered; the tonic pattern is related to the muscle tone whereas the phasic one is related to the motor activity. In AS, muscle tone is often inhibited, giving way to a phasic activity.

Sleep and respiratory control During QS, the breathing is mainly under metabolic control, through chemoreceptors (central and peripheric), integrated in bulbo-protuberantial centers. Cortical connections are inactived and few motor perturbations disturb the respiratory control during this state.
During AS, the breathing is mainly under control of a specific system, called "AS-state", where tonic and phasic systems coexist. Some specific bulbo-protuberantial AS-neurons (non respiratory neurons) are supposed to change the activity of the spinal respiratory neurons, through tonic impulsions. The phasic system modifies this background activity to adapt the respiratory control to the current movements. There is an inhibition of the hypothalamic control mechanisms and an exclusive influence of these brainstem neurons. This inhibition is thought to be responsible for a loss in the efficiency of the homeostasic regulations during AS [38].
These differences in the regulation mechanisms could explain why the differences in RSA are expressed in QS and not in AS: QS is the state where the bulbo-protuberantial interaction between the respiratory center and the vagus center can be the strongest, producing the RSA (vagal inhibition synchronised with firing of inspiratory motoneurons), whereas in AS these interactions are permanently modified. Morever, the QS is supposed to be particularly vulnerable in the first year of life because of the transition from one to four stages [9], during this particular epoch of human ontogenesis.

Sleep and cardiovascular control During QS, there is a high cardiovascular stability, with a slower heart rate due to the negative chronotropic effect of a dominant parasympathetic tone and a subsequent diminution of the arterial blood pressure without change in peripheral resistances.
During AS, the cardiovascular regulation is more important, fluctuations of arterial blood pressure and heart rate often arise , according to phasic events. These fluctuations can be explained by the opposed effects of the tonic and phasic states:

during tonic AS, there is a global diminution of heart rate, arterial blood pressure and peripheral resistances, through a strong central sympathetic inhibition. On the opposite, during phasic AS, an increase in the vasoconstriction in skeleton muscles through an increase in sympathetic tone gives an increase in heart rate, arterial blood pressure and peripheral resistances.
Some experiments of sino-aortic denervation in the cat (Guazzi and Zancheti, cited in [38]) show the important role of the baroreflex in the cardiovascular control during AS: especially the phasic events give a very high instability of the arterial blood pressure, sometimes incompatible with a correct cerebral circulation. It seems that baroreflex are essential in cardiovascular regulation during AS and that the Nucleus Tractus Solitarius, first relay and integration center, is a very important structure for this homeostasic balance.
These differences in the regulation mechanism could explain why the differences in baroreflex activity between control and anemic infants are expressed in AS and not in QS: AS is the state where the baroreflex is the most evidently solicited, and so an abnormality can be better seen in AS than in QS.
One can make the assumption that anemic subjects show a delay in maturation of the cardiovascular control, with an instability of the baroreflex response, responsible for a higher activity in the range of the Mayer waves. However, as this higher activity could be only consecutive to an increase of the motor activity in the anemic group, we can't really conclude in favour of an abnormality but only in a higher solicitation of the baroreflex regulation.

7.3.2 Hypothesis on mechanisms underlying iron deficiency

Iron is involved in lipid metabolism and is thought to have a role in production and maintenance of myelin, as it has been shown in the rat, for which a restriction in iron leads to poor myelination [41]. This default, which alters neurotransmission, could affect parasympathetic fibers, entirely and late myelinated in postnatal period, and the sympathetic fibers myelinated on their pre-ganglion traject [42, 43]. It could explain both the effect on the RSA in QS and the effect on the baroreflex regulation in AS.
The results suggest a delayed or abnormal development of the ANS in anemic infants: smaller parasympathetic tone in QS, stronger baroreflex excitability in AS. Furthemore, the poor differentiation of heart rate variability parameters according to sleep states in the anemic group reinforces this hypothesis. A reduced SNA activity, especially of the vagal tone, could affect infants in an important way, in so far as ANS integrity is essential for a correct organization of physiological resources, for

an appropriate response to stress, for a good interaction of cardiovascular and respiratory control with sleep-waking states. This could contribute to poorer behavioral and developmental outcomes in anemic infants.

8 Conclusion

The use of the DWT is well suited for its good frequency resolution in low frequencies. Yet, it provides only a dyadic decomposition, which is inherent in the discretisation process; one might get better accuracy on the physiological frequency bands by performing continuous wavelet transform.
This study allows us to point out some physiological results which add further evidence to a delayed or abnormal ANS development in anemic infants. This suggests that iron is an essential micronutriment for the normal development of the autonomic control system.

Acknowledgments

This study received financial support by grants from Fondecyt 1940467 (CONICYT, Chile), NIH R01 HD14122, ECOS/CONICYT.

References

[1] Florentino RF, Guirriec RM (1984): Prevalence of nutritional anemia in infancy and childhood with emphasis on developing countries. In *Steckel A (ed) Iron Nutrition in Infancy and Childhood.* Raven Press, New York, pp61-74.

[2] Huratdo EK., Scott KG., Claussen AH., Boussy CA., Goozis K (1995): Long term effects of iron deficiency on child development. In *Society for Research in Child development, abstracts.*

[3] Fox NA., Porges SW (1985) The relation between neonatal period heart period patterns and developmental outcome. *Child Dev*, 56:28-37.

[4] Curzi-Dascalova L., Spassov L., Eiselt M., Peirano P. Kauffmann F., Clairambault J.,Médigue C. (1994): Development of cardiorespiratory controla and sleep in newborns. In *Cosmi AV, renzo GC (eds) Current progress in Perinatal medicine.* Parthenon Publishing group, London, pp 303-308.

[5] Novak V., Novak P., De Champlain J., Le Blanc R., Martin R. and Nadeau R. (1993): Influence of respiration on haert rate and blood pressure fluctuations; *The American Physiological Society*, p 617-626.

[6] P. Novak, V. Novak *"Time/frequency mapping of the heart rate, blood pressure and respiratory signals"* Med. and Biol. Eng. and Comp., p. 103-110, 1993.

[7] Lozoff B., Wolf AW., Urrutia JJ, Viteri FE (1985): Abnormal behavior and low developmental test scores in iron-deficient anemic infants. *J Dev Behav Pediatr*, 6:69-75.

[8] Peirano P., fagioli I., Bes F., Salzarulo P (1993): The role of slow-wave sleep on the duration of quiet sleep in infants. *j Sleep res*,2:130-133.

[9] Peirano P., Fagioli I., Singh BB., Salzarulo P (1989): Effect of early human malnutrition on waking and sleep organization. *Earlu Hum Dev*, 20:67-76.

[10] S. G. Mallat: Multiresolution Approximations and Wavelet Orthonormal Bases for $L^2(\mathbb{R})$, *Trans. Amer. Math. Soc.*, vol. 315, No. 1, pp. 69-88, 1989.

[11] I. Daubechies: Ten Lectures on Wavelets.

[12] P. P. Vaidyanathan: Quadrature Mirror Filter Banks, M-Band Extensions and Perfect Reconstruction Techniques, *IEEE ASSP MAGAZINE*, July 1987.

[13] Benveniste, A. and Berry, G. (1991): The Synchronous Approach to Reactive and Real-Time Systems.*Proceedings of the IEEE* vol79, n.9, 1270-1282.

[14] R.D. Berger, S. Akselrod, D. Gordon, R.J. Cohen *"An efficient algorithm for spectral analysis of heart rate variability"* IEEE Trans. on Biomed. Eng., vol BME33, no 9, p. 900-904, 1986.

[15] Bestel, J. (1994): Etude de méthodes temps-fréquence appliquées au Rythme Cardiaque développées en langage synchrone Signal, *rapport de stage seconde année, ICPI-CPE Lyon, section électronique et traitement de l'information*, septembre 1994.

[16] Clairambault, J., Curzi-Dascalova, L., Kauffmann, F., Médigue, C., Leffler, C. (1992): Heart Rate Variability in normal sleeping full-term and preterm neonates. *Early Human Development*, 28, 169-183.

[17] McCloskey DI. (1994): *Vagal Control of the Heart: Experimental Basis and Clinical Implications*, Ch.5:65-72.

[18] Le Guernic, P., Gautier. T., Le Borgne, M. and Le Maire, C. (1991): Programming Real-Time Applications with SIGNAL. *Proceedings of the IEEE* vol79, n.9, 1321-1336.

[19] Médigue, C., Dupont, F., Clairambault, J., Curzi-Dascalova, L., Spassov, L. (1992): A Synchronous Language, SIGNAL: application to Heart Rate Variability and Body Movements Analysis in Sleeping Newborns. In: *Computers in Cardiology 1992*, 471-474.

[20] Médigue, C., Clairambault, J., Curzi-Dascalova, L. (1992): A real time heart rate variability analysis system using a synchronous language: Signal. In: Actes de la 14^{e} conférence annuelle internationale de l'*IEEE Engineering in Medicine and Biology Society*, 766-767, Paris, octobre 1992.

[21] Médigue, C., Clairambault, J., Kauffmann, F., Sorine, M., Curzi-Dascalova, L. (1992): Utilisation du langage SIGNAL pour l'étude d'algorithmes de traitement du signal électrocardiographique. *Rapport de Recherche INRIA* n^{o} 1717.

[22] Merri, M., Farden, D.C., Mottley, J.G., Titlebaum, E.L. (1990):Sampling Frequency of the Electrocardiogram for Spectral Analysis of the Heart Rate Variability, *IEEE Transactions on Biomedical Engineering*, vol. 37, n^{o}. 1, January 1990.

[23] J. Pan, W.J. Tompkins *"A real-time QRS detection algorithm"* IEEE Trans. on Biomed. Eng., vol BME32, no 3, p. 230-236, 1985.

[24] Saul, JP., Cohen, RJ (1994): respiratory Sinus Arrhytmia. *Vagal Control of the Heart: Experimental Basis and Clinical Implications*; MN Levy, PJ Schwartz eds. Futura Publishing Co.Inc.Armonk,NY.

[25] Thames MD., Dibner-Dunlap ME., Smith ML. (1994):*Vagal Control of the Heart: Experimental Basis and Clinical Implications*, Ch.23:369-378.

[26] Vermeiren, C. (1993): Etude de méthodes temps-fréquence dans le langage synchrone SIGNAL appliquées aux signaux biomédicaux. Rapport de stage de DEA de Génie Biologique et Médical (Université de Créteil) effectué à l'INRIA-Rocquencourt, Créteil, septembre 1993.

[27] Vermeiren, C., Médigue C., Krouma, A., Bestel J. (1994): LARY_C : logiciel d'Analyse des Rythmes Physiologiques pour l'étude du Système Nerveux Autonome. *Rapport technique INRIA*,n^o 0166.

[28] Vermeiren, C., Médigue C., Clairambault, J., Curzi-Dascalova, L. (1994): Beat-to-beat cardio-respiratory demodulation. In: Actes de l'*IFAC Symposium on modelling and control in biomedical systems*, 142-143, Galveston, TX, mars 1994.

[29] Vermeiren, C., Escourrou P., Papelier Y., Le Vey Georges., Przybyszewski A.W. (1995): Assessment of the phase relationship between breathing, heart rate and blood pressure by the modified complex demodulation. In : *Actes de la 17^e conférence internationale annuelle de l' IEEE Engineering in Medicine and Biology Society*,pages 943-944, Montréal, septembre 1995.

[30] Médigue, C., Vermeiren, C., Bourgin P., Debouzy C., Escourrou P. (1995): Cardiovascular Perturbations involved in Periodic Leg Movements In: *Proceedings of Computers in Cardiology 1995*, pages. Congrès annuel de *Computers in Cardiology*, pages 477-480, Vienne, Autriche, septembre 1995.

[31] Mansier P, Médigue C, Charlotte N, Vermeiren C, Coraboeuf E, Deroubai E, Clairambault J, Carré F, Dahkli T, Bertin B, Briand P, Strosberg and Swynghedauw B (1996): Decreased heart rate variability in transgenic mice overexpressing atrial β1-adrenoreceptors. *American Journal of Physiology*, p 1465-1472 (1996).

[32] Médigue, C., Vermeiren, C., Garrido, M., Peña, M., Peirano, P. (1996): Assessment of autonomic dysfunction in iron-deficient anemic infants by cardio-respiratory demodulation. In : *Actes de la 18e conférence internationale annuelle de l' IEEE Engineering in Medicine and Biology Society*, p 336-337, Amsterdam, 31 oct. - 3 nov. 1996.

[33] Vermeiren, C. (1996): Analyse et modélisation du système cardio-vasculaire et sa régulation à court terme par le système nerveux autonome. Thèse en Génie Biologique et Médical, Université de Paris Val de Marne (Paris XII).

[34] Eiselt, M., Curzi-Dascalova, L., Clairambault, J., Kauffmann, F., Médigue, C., Peirano, P. (1993): Heart-rate variability in low-risk prematurely born infants reaching normal term: a comparison with full-term newborns. *Early Human Development*, 32, 183-195.

[35] Spassov, L., Curzi-Dascalova, L., Clairambault, J., Kauffmann, F., Médigue, C., Peirano, P. (1994): Heart rate and heart rate variability in small-for-gestational-age newborns. *Pediatric Research*, 35, 500-505.

[36] Krzzanowski WJ., 1977: The performance of Fisher's linear discriminant function under non optimal conditions. *Technometrics*, 19,191-200.

[37] Lachenbruch PA, 1975: Discriminant analysis, Ch. 7, *Hafner Press*, MacMillan Publishing Co.

[38] Laguzzi R. (1992): Sommeil et régulations neurovégétatives chez l'animal; dans: *Le sommeil humain. Bases expérimentales et physiopathologiques*, O. Benoit et J. Foret, châp. 4, p 33-44; Ed. Masson.

[39] Kurtz D. (1992): Sommeil et fonctions cardio-circulatoires; dans: *Le sommeil humain. Bases expérimentales et physiopathologiques*, O. Benoit et J. Foret, châp. 12, p 139-145; Ed. Masson.

[40] Curzi-Dascalova, L., Mirmiran Majid (1996): Manual of methods for recording and analysing sleep-wakefulness states in preterm and full-term infant. In *Techniques en ...*, Ed. INSERM.

[41] Larkin E.C., Rao G.A. (1990): Importance of fetal and neonatal iron: Adequacy for normal development of central nervous system. In *Dobbing J (ed) Brain, Behaviour, and Iron in the Infant Diet.* Springer-verlag, London, pp 43-62.

[42] Pereyra PM, Zhang W, Schmidt M, Becker LE, (1992): Development of myelinated and unmyelinated fibers of human vagus nerve during the first year of life. *J Neurologic Sci*; 10:107-113.

[43] Sarnat HB, Netsky MG (1981): Evolution of the Nervous System; *ed 2. Oxford University Press*, New York.

Unit´e de recherche INRIA Lorraine, Technopôle de Nancy-Brabois, Campus scientifique,
615 rue du Jardin Botanique, BP 101, 54600 VILLERS LÈS NANCY
Unit´e de recherche INRIA Rennes, Irisa, Campus universitaire de Beaulieu, 35042 RENNES Cedex
Unit´e de recherche INRIA Rhône-Alpes, 655, avenue de l'Europe, 38330 MONTBONNOT ST MARTIN
Unit´e de recherche INRIA Rocquencourt, Domaine de Voluceau, Rocquencourt, BP 105, 78153 LE CHESNAY Cedex
Unit´e de recherche INRIA Sophia-Antipolis, 2004 route des Lucioles, BP 93, 06902 SOPHIA-ANTIPOLIS Cedex

Éditeur
INRIA, Domaine de Voluceau, Rocquencourt, BP 105, 78153 LE CHESNAY Cedex (France)
http://www.inria.fr
ISSN 0249-6399